

The Bent Hawaiian-Emperor Hotspot Track: Inheriting the Mantle Wind

John Tarduno,^{1,2*} Hans-Peter Bunge,³ Norm Sleep,⁴ Ulrich Hansen⁵

Bends in volcanic hotspot lineaments, best represented by the large elbow in the Hawaiian-Emperor chain, were thought to directly record changes in plate motion. Several lines of geophysical inquiry now suggest that a change in the locus of upwelling in the mantle induced by mantle dynamics causes bends in hotspot tracks. Inverse modeling suggests that although deep flow near the core-mantle boundary may have played a role in the Hawaiian-Emperor bend, capture of a plume by a ridge, followed by changes in sub-Pacific mantle flow, can better explain the observations. Thus, hotspot tracks can reveal patterns of past mantle circulation.

The Hawaiian-Emperor track (Fig. 1) is the archetype used to illustrate plate motion over a hotspot. In the classic view, volcanism on the surface recorded regular plate motion over a plume deep within Earth's mantle that produced a fixed region of melting near the surface (hotspot). The great bend separating the northwestern-trending Hawaiian chain from the north-south-oriented Emperor Seamounts was thought to trace a $\sim 60^\circ$ change in absolute plate motion. However, a paleomagnetic test based on ocean drilling in 2001 revealed that the islands and seamounts had formed at different latitudes (1). The Emperor trend seamounts thus record motion of the upwelling in the mantle.

Why didn't the community accept hotspot mobility earlier? The elegant and captivating geometry of the fixed hotspot idea (2) compelled a search for alternatives to emerging contradictory findings. It had been recognized in reconstructing plate motions that a fixed Hawaiian hotspot was inconsistent with fixed hotspots in the Indo-Atlantic realm (3). However, early reconstructions relied on a critical plate circuit link through the then poorly understood Antarctic and southernmost Pacific region. The possibility of undocumented plate motions provided an option that avoided hotspot drift. Paleomagnetic data from a single Pacific site also indicated hotspot motion, but they could be interpreted as a record of polar wander (4), the rotation of the entire solid Earth in response to shifts in its mass heterogeneities. In addition, although plumes could easily have been envisioned as swaying in the mantle, the geodynamic details were wanting.

¹Department of Earth and Environmental Sciences, University of Rochester, Rochester, NY 14627, USA. ²Department of Physics and Astronomy, University of Rochester, Rochester, NY 14627, USA. ³Department of Earth and Environmental Sciences, Ludwig-Maximilians Universität, München, 80333 München, Germany. ⁴Department of Geophysics, Stanford University, Stanford, CA 94305, USA. ⁵Institut für Geophysik, Universität Münster, 48149 Münster, Germany.

*To whom correspondence should be addressed. E-mail: john@earth.rochester.edu

Two premises embedded in the dynamic equations of how the mantle moves preclude stationary hotspots. The first is the principle of mass conservation: Any plate movement at the surface must be balanced by motion deeper in the mantle. The second premise is that the mantle can be taken as a highly viscous fluid—a nominal viscosity of 10^{21} Pa·s is suggested from studies of postglacial rebound (5). The large mantle viscos-

ity implies that velocity gradients are small and that inertial forces pale in comparison to viscous ones; thus, the mantle transmits stresses nearly instantaneously. Given both premises, any plate motion change must go along with changes in the internal mantle flow. Hager and O'Connell (6) used this insight to infer deep mantle motion from the surface plate tectonic pattern in the decade following the first use of a hotspot reference frame.

Subsequent advances in seismic tomography and past plate motion modeling allowed modeling of the temporal evolution of the mantle back in time. Steinberger and O'Connell (7) produced a synoptic view of past mantle circulation that suggested southward motion of the Hawaiian hotspot, consistent with paleomagnetic data (8). Geophysical cruise results and paleomagnetic studies resolved potential gaps in plate circuits [e.g., (9, 10)], and global paleomagnetic tests excluded polar wander (11–13). These developments have set the stage for a reassessment of mantle processes that could be recorded by large bends in hotspot tracks.

An Alternative Hawaiian-Emperor Track

To visualize the implications of hotspot motion, we consider what the Hawaiian-Emperor track

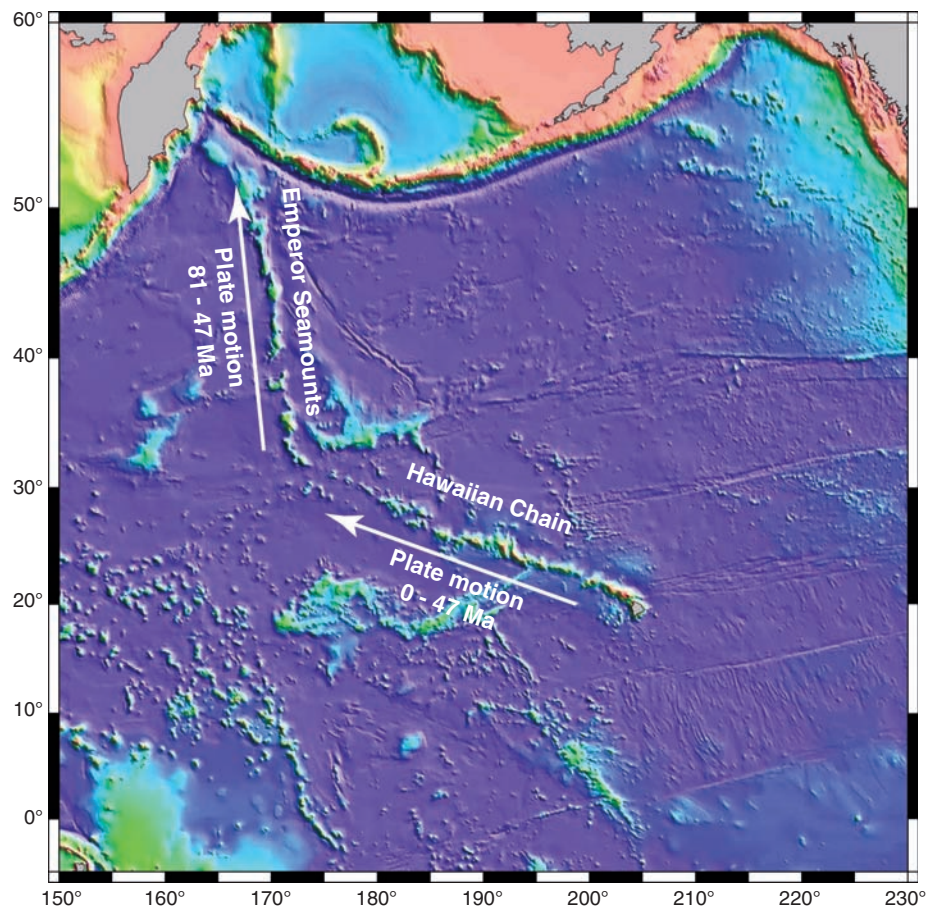


Fig. 1. Bathymetry of the northwest Pacific Ocean basin. The traditional interpretation is highlighted: The Hawaiian volcanic chain records absolute Pacific plate motion to the northwest, whereas the Emperor Seamounts reflect a more northerly plate direction.

might have looked like had the Hawaii hotspot actually been fixed relative to the deep mantle. To do this, we use plate circuits and assume that volcanic chains in the Indo-Atlantic realm reflect fixed hotspots. These predictions are thus still not free of the fixed hotspot hypothesis, but paleomagnetic studies suggest that the hotspots in the Indo-Atlantic have not moved much since the Late-Cretaceous-Paleogene, when the Emperor Seamounts were formed (14).

The plate circuit that traverses the Indo-Atlantic and Pacific realms via Antarctica (9, 14) yields a hypothetical trace that is similar to the Hawaiian chain for the last ~30 million years (Fig. 2, A to C). For older times, differences build. The Hawaiian-Emperor bend of the extant track is replaced by a gentle ~30° of curvature in the hypothetical trace (Fig. 2D). This moderate curvature is similar to that seen in the Louisville chain, the other hotspot track from the Pacific Ocean basin with a long, clear age progression (15) that is not confused by lithospheric structure. Moreover, the hypothetical trace resembles an oceanic fracture zone, a feature of Earth's surface known to record plate motion over tens of millions of years (16). As is the case with fracture zones, we can fit the trace with several small circle segments, the junction of each representing a change in plate motion. The bend in the actual track might represent one of these junction times in the hypothetical trace.

An alternative plate circuit involves transfer from Antarctica to Australia, and then through Lord Howe Rise (Fig. 2, B and C). In the predictions arising from use of this circuit, a somewhat sharper bend remains, which could imply a larger plate motion change (17). Both plate circuits pass paleomagnetic consistency tests (14); we cannot distinguish between them with the resolution of the available data. However, while avoiding the Antarctic-Pacific connection, the second circuit relies on a contentious assumption: Lord Howe Rise is locked to the Campbell Plateau between 84 and 47 million years ago (Ma). Moreover, when a revised history of Antarctic-Australian spreading history (18) is incorporated into the circuit through Lord Howe Rise, the predictions for the locations of the Hawaiian-Emperor chain (Fig. 2C) converge to those derived from the Antarctic connection (19). Both plate circuits indicate that the large present-day latitudinal trace of the Emperors is mainly due to hotspot drift, consistent with the

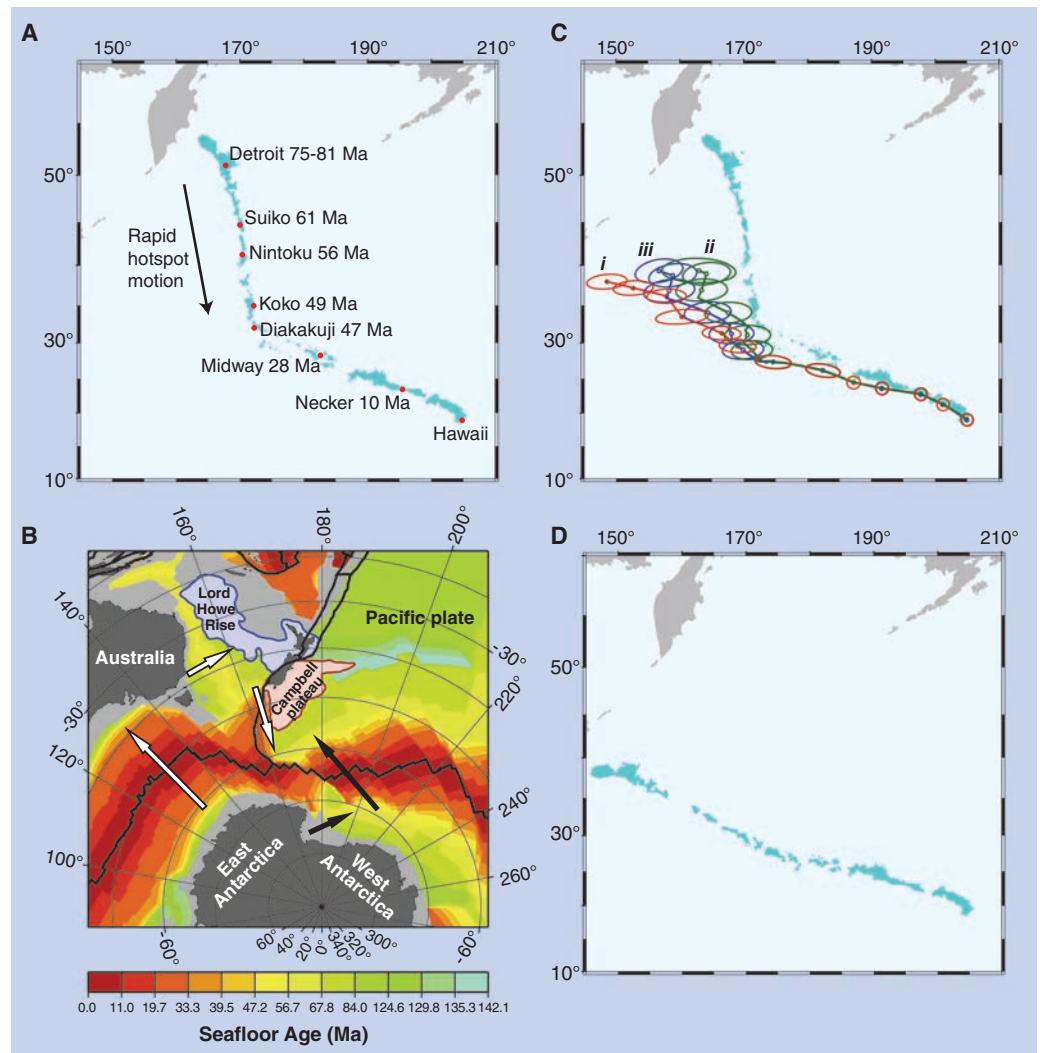


Fig. 2. Alternative Hawaiian-Emperor traces. **(A)** Present-day track with ages and episode of rapid hotspot motion highlighted. **(B)** Differences in how plate circuits connect the Indo-Atlantic realm to the Pacific for Late Cretaceous to middle Eocene times [from (14)]. In the standard reconstruction [e.g., (9)], the connection is through East-West Antarctica (black arrows); in a more recent circuit, the connection is through Australia and the Lord Howe Rise (white arrows) (17). **(C)** Predicted tracks from plate circuits [see (14) and (19) for ages and uncertainty analysis]: (i) East-West Antarctica circuit (red); (ii) Australia-Lord Howe Rise circuit (green); (iii) Australia-Lord Howe Rise circuit modified with a revised Antarctic-Australia spreading history [from (17)] (blue). Note that path (iii) converges to path (i). **(D)** Trace that would have been produced had the Hawaiian hotspot been fixed in the deep mantle (16). Predictions based on East-West Antarctica circuit.

paleomagnetic determinations from ocean drilling (1, 8).

Candidate Processes

Two models have been proposed to explain hotspots. One is a “top-down” plate-driven process in which rifting of the lithosphere stimulates shallow mantle melting (20). The second is a “bottom-up” model in which an upwelling or plume (2) rises in the mantle from a thermal boundary layer (the transition zone at ~700 km or as deep as the core-mantle boundary). Seismic data are still inconclusive, but we favor and thus explore the mantle plume explanation for Hawaiian volcanism in which a long-lived, narrow upwelling from the deepest mantle episodically constructs volcanic islands and seamounts. The Hawaiian hotspot’s

large volume flux (~350 m³ s⁻¹) (21), spatial pattern, and longevity are best explained by the mantle plume hypothesis. Some studies of alternative mechanisms (e.g., a propagating crack) show that they are inadequate (21), whereas other modeling has shown that deep mantle plumes contribute substantially to the mantle energy budget (22). Below, we identify five physical processes that could have caused hotspot motion and the Hawaiian-Emperor bend. We use 47 Ma as the best age for the bend; an older age of 50 million years has been proposed (23), but this relies on a relocation of the bend 200 km north of the typical feature on the sea floor (16).

1) Ridge interaction and asthenospheric flow. Plumes will impinge at the base of the lithosphere; ponded material can flow in a type of

upside-down drainage toward a ridge (24). Plate reconstructions (25, 26) and geochemical data (27) indicate that a ridge lay north of Detroit Seamount during its construction. Hence the hotspot, perhaps once located to the south, may have been “pinned” by the more northerly ridge (Fig. 3A). The mid-ocean ridge basalt signature seen in Detroit Seamount lavas is not seen in the younger Suiko Seamount (27). Thus, we infer that this shallow flow influenced the formation of only the northernmost seamounts (i.e., Detroit Seamount and Meiji Guyot) of the Emperor track (1).

2) Ridge upwelling and deeper mantle flow. Upper mantle flow is more rapid near mid-ocean ridges, and numerical modeling suggests that considerable tilts of the deeper plume conduits toward ridges might begin at depths of 1200 to 1500 km (Fig. 3B). Scaling arguments (28) limit the distance over which plumes and ridges interact to about 1500 km. Plate reconstructions show that a number of ridges have crossed the Pacific since 140 Ma at velocities of several centimeters per year (29). Thus, this ridge migration could have captured mantle plumes through flow directed at the ridge. If the ridge moves beyond that distance, a captured plume would presumably return to its original location over a deep mantle source.

3) Advection of the plume conduit and entrainment in the mantle wind. As a plume rises through the mantle, the plume conduit can be tilted as mantle convection continues over time (Fig. 3C), moving where it interacts with the shallow mantle and crust, giving rise to drift observed at the surface (7). Models of this process have been successful in explaining the first-order paleomagnetic observations (1). The apparent velocity of the hotspot can be twice that of the mantle circulation component. If the tilt becomes too great, the conduit may lose consistency. However, in most models, the tilted thermal plumes do not break up into a series of diapirs. Rather, small-scale convection near the plume conduit can entrain material from the surrounding mantle (30). This process readily disrupts tilted isoviscous plumes, but laboratory and theoretical studies suggest that tilted plumes with strongly temperature-dependent viscosities and fluxes appropriate to the mantle remain intact and do not entrain much surrounding material (31, 32).

4) Movement of the plume base: influence of a superplume. Hawaii is an outlier relative to the cluster of hotspots in the South Pacific, a region that was anomalous in the Cretaceous when the Mid-Pacific Mountains and other seamounts formed (11, 33). Modeling shows that the base of a plume tends to move toward a broad upwelling (34) (Fig. 3D). This process might be especially important if the plume arises from a tabular upwelling; the plume source could conceivably move along-strike of the larger upwelling. Lateral heterogeneity in D’ implies that some regions, such as “cusps” where dense material has been entrained, might serve to anchor the plume source (35). Together, these processes

could account for differences in the motion histories between plumes and the temporal character of movement exhibited by a single plume such as Hawaii.

5) Mantle convection coupled to plate motion change. The paleomagnetic data from the Emperor Seamounts imply that there was a major change in the nature or vigor of mantle convection in the Pacific at 47 Ma, because the present-day latitude of the hotspot and paleolatitude estimates of islands, atolls, and seamounts back to the bend are similar (1). Plate motion-driving forces for this change include initiation of subduction in the Izu-Bonin arc and ridge subduction in the northwestern Pacific (18), events that may have commenced at (or before) 50 Ma (23).

However, it is also possible that other far-field plate tectonic changes could have a cumulative effect that is not adequately captured by the current generation of plate and mantle flow models.

Scales of Hotspot Motion and Mantle Convection

In further assessing the physical processes that potentially created the bend, we consider first the background mantle motion. Geochemistry (36), seismic tomography (37, 38), the geoid (39), the distribution of hotspots (40), and the history of subduction (41) suggest a flow pattern organized with two major upwellings under the Pacific and Africa, separated by a great circle of downwelling surrounding the Pacific. Although fluid

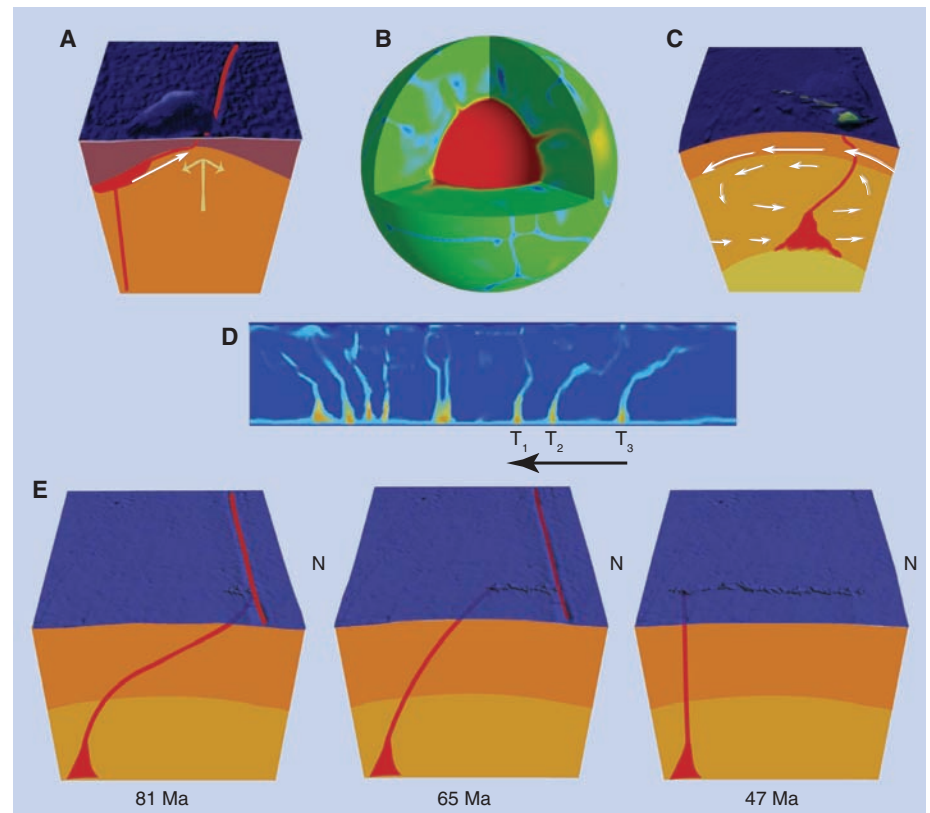


Fig. 3. Hotspot drift related to shallow (A), mid-mantle (B and C), and deep-mantle (D) processes. (A) Hotspot volcanism is channeled to a nearby ridge by asthenospheric flow (schematic) (see (1, 24) for discussion). (B) Superadiabatic temperatures for a three-dimensional spherical mantle convection model with depth-dependent viscosity and bottom heating [from (42)]. The uppermost 200 km of the mantle is removed to show the temperature distribution beneath the thermal boundary layer. Large horizontal flow velocities in the asthenosphere, directed at an upwelling (ridge), result in a strongly tilted plume conduit. (C) Advection of plume conduits, tilted by mantle flow (schematic). See (1, 7, 17) for model results for Hawaii and other hotspots. (D) Movement of the base of a plume influence by a large-scale upwelling following (34). A composite snapshot of the model is shown, displaying the evolution of the temperature field in a convecting mantle. Material properties are assumed to depend on pressure and temperature. The coefficient of thermal expansivity decreases by a factor of 10 from top to bottom; the viscosity increases sharply with pressure and decreases with temperature. The Rayleigh number, based on surface values of viscosity and expansivity, was set to 10^7 . The original experiment was conducted in a wide box (aspect ratio 36) to minimize edge effects. Here, the box has been truncated to highlight the phenomenon of plume movement. T1, T2, and T3 represent subsequent position of a hotspot as its base moves toward a central upwelling. (E) Schematic of one plume capture and release scenario for the Hawaiian-Emperor chain. The plume is bent between 1200- and 1500-km depth toward the mantle upwelling associated with the Pacific-Kula ridge system at 81 Ma; upwelling abates thereafter, allowing the plume to return to its original position relative to the deep mantle by 47 Ma.

dynamic theory of an isoviscous mantle predicts shorter convective length scales on the order of the mantle depth, modeling (42) and analytic studies (43) indicate that the larger-scale structure is a robust property of mantle flow having a low-viscosity channel, or asthenosphere.

The asthenosphere decouples plate movement from deeper mantle motion. Modeling shows that the decoupling is proportional to the inverse of the natural logarithm of the viscosity contrast between the upper and the lower mantle (44). Overall, the rate of mantle wind scales with slab descent rate (45). Mantle circulation simulations (46) predict deep mantle flow velocities on the order of 1 cm/year for mantle viscosity contrasts of 10 to 100 (47). Thus, it is possible to reconcile both times of near-hotspot fixity and times of hotspot movement with vigorous plate motion [e.g., (48)]. The longest spatial scale of convection implies that hotspots might move as groups (11). In fact, when paleomagnetic data from the Indo-Atlantic region are referenced to hotspots of that area, and paleomagnetic data from the Pacific are tied to its hotspots, there is a discrepancy (11–13, 16). This was once thought to be a sign of polar wander (49), even though such polar shifts are small in mantle convection models with an asthenosphere (50). The difference is now recognized as a signal of hotspot motion and large-scale ($l = 2$) mantle convection (11, 51).

Mantle circulation models also predict that deep mantle motion in the Late Cretaceous, when plate velocities were about twice as fast as they are today, did not exceed 2 cm/year. Rapid hotspot movement, comparable to the rates seen for Hawaii at the time between 81 and 47 Ma (>4 cm/year), is thus unlikely to originate solely from deep mantle processes. Fast-velocity episodes could instead arise in the shallow mantle, where flow velocities are large. Hotspot bends, and changes between periods of fast and slow plume motion, may then signal the switch between flow regimes in the shallow and the deeper mantle, respectively.

Models involving plume capture by a ridge are of special relevance for the Hawaiian-Emperor chain because the large shallow mantle flow rates are concomitant with the high hotspot drift rates (1). When spreading rates are slow, such as in the Atlantic, the mantle flow may be so weak that hotspots can cross ridges (48). In the faster-spreading Pacific ridges, mantle wind can produce more plume tilt.

Moreover, plume capture is consistent with two key traits of the chain and Pacific basin tectonic history. First, the scaling considerations yield a limit on the lateral extent of fast plume motion of about 15° ; that is the maximum distance from which a captured plume could return to its original location. Drift models based on paleomagnetic data from the Emperor Seamounts (1) suggest that the rapid phase of Hawaiian hotspot motion covered 11° to 15° of latitude. Second, the Hawaiian hotspot was close to a fast-spreading ridge [full rate estimated as 180 mm

year⁻¹ (21)] at 75 to 81 Ma, but spreading ceased sometime between 56 Ma and the age of the bend (52). Ridge transforms and jumps [e.g., (26)] will complicate patterns of upwelling. The Emperor Seamounts may record an interval tens of millions of years long when the large-scale mantle upwelling associated with the Kula–Pacific ridge system north of the Hawaiian hotspot waned. This progressive change, possibly with other tectonic events on the paleo-Pacific margin [e.g., (18)], would have reduced any northward sub-Pacific mantle flow, allowing the captured plume to return to its original position in a dominant southward flow (1, 7). Since this shift, the hotspot has been far from ridge influences and relatively stable, reflecting deeper and more sluggish mantle flow.

Further Resolution

Mantle flow models are about to achieve the numerical resolution needed (100 million to 1 billion grid points) to represent the vigor of global mantle flow, allowing further testing of plume capture. Incorporation of constraints from mineral physics [e.g., (53)] is improving models, and assimilation of refined seismic tomography and plate-motion histories is helping to overcome the limitations of unknown initial conditions (54). New observations can help. The Hawaiian-Emperor chain is well suited for paleomagnetic tests because its track is narrow. In other cases, such as Cretaceous hotspots on the Indian plate, locations are uncertain because of the >1000 -km spatial scale of magmatism (commonly attributed to mantle plume heads). Drilling of the Emperor Seamounts was designed to test whether the Hawaiian hotspot had moved (1). Deeper drilling is needed to obtain the paleolatitude resolution required to investigate temporal variations in hotspot drift (16). Intrabasin hotspot motion can be assessed by drilling the Louisville hotspot track (15). The motion histories of Indo-Atlantic hotspots with narrow tracks can be evaluated by paleomagnetic analyses of continental rocks; when compared with Pacific data, these histories provide a means to gauge motion of hotspot groups. These efforts should ultimately allow the community to use hotspot tracks and their bends as measures of past mantle flow.

References and Notes

1. J. A. Tarduno *et al.*, *Science* **301**, 1064 (2003).
2. W. J. Morgan, *Geol. Soc. Am. Mem.* **132**, 7 (1972).
3. P. Molnar, T. Atwater, *Nature* **246**, 288 (1973).
4. W. J. Morgan, in *The Sea*, C. Emiliani, Ed. (Wiley, New York, 1981), vol. 7, pp. 443–487.
5. J. X. Mitrovica, *J. Geophys. Res.* **101**, 555 (1996).
6. B. H. Hager, R. J. O'Connell, *J. Geophys. Res.* **84**, 1031 (1979).
7. B. Steinberger, R. J. O'Connell, *Geophys. J. Int.* **132**, 412 (1998).
8. J. A. Tarduno, R. D. Cottrell, *Earth Planet. Sci. Lett.* **153**, 171 (1997).
9. S. C. Cande, C. A. Raymond, J. Stock, W. F. Haxby, *Science* **270**, 947 (1995).
10. V. DiVenere, D. V. Kent, *Earth Planet. Sci. Lett.* **170**, 105 (1999).
11. J. A. Tarduno, J. Gee, *Nature* **378**, 477 (1995).

12. J. A. Tarduno, A. V. Smirnov, *Earth Planet. Sci. Lett.* **184**, 549 (2001).
13. T. H. Torsvik, R. Van der Voo, T. F. Redfield, *Earth Planet. Sci. Lett.* **202**, 185 (2002).
14. P. V. Doubrovine, J. A. Tarduno, *J. Geophys. Res.* **113**, B071104 (2008).
15. A. A. Koppers, R. A. Duncan, B. Steinberger, *Geochem. Geophys. Geosyst.* **5**, Q06102 (2004).
16. J. A. Tarduno, *Chem. Geol.* **241**, 234 (2007).
17. B. Steinberger, R. Sutherland, R. J. O'Connell, *Nature* **430**, 167 (2004).
18. J. M. Whittaker *et al.*, *Science* **318**, 83 (2007).
19. P. V. Doubrovine, J. A. Tarduno, *J. Geophys. Res.* **113**, B121101 (2008).
20. D. L. Anderson, *Geophys. Res. Lett.* **27**, 3623 (2000).
21. N. H. Sleep, in *Plates, Plumes and Planetary Processes*, G. R. Foulger, D. M. Jurdy, Eds. (GSA Spec. Pap. 430, Geological Society of America, Boulder, CO, 2007), pp. 29–45.
22. H.-P. Bunge, *Phys Earth Planet Int.* **153**, 3 (2005).
23. W. D. Sharp, D. A. Clague, *Science* **313**, 1281 (2006).
24. N. H. Sleep, *J. Geophys. Res.* **101**, 28065 (1996).
25. R. D. Cottrell, J. A. Tarduno, *Tectonophysics* **362**, 321 (2003).
26. I. O. Norton, in *Plates, Plumes and Planetary Processes*, G. R. Foulger, D. M. Jurdy, Eds. (GSA Spec. Pap. 430, Geological Society of America, Boulder, CO, 2007), pp. 451–470.
27. R. A. Keller, M. R. Fisk, W. M. White, *Nature* **405**, 673 (2000).
28. N. Ribe, *J. Geophys. Res.* **101**, 16,195 (1996).
29. R. D. Müller, M. Sdrolias, C. Gaina, W. R. Roest, *Geochem. Geophys. Geosyst.* **9**, Q04006 (2008).
30. M. A. Richards, R. W. Griffiths, *Nature* **342**, 900 (1989).
31. R. C. Kerr, C. Meriaux, *Geochem. Geophys. Geosyst.* **5**, Q12009 (2004).
32. N. H. Sleep, *Geochem. Geophys. Geosyst.* **8**, Q11005 (2007).
33. J. A. Tarduno, W. W. Sager, *Science* **269**, 956 (1995).
34. U. Hansen, D. A. Yuen, S. E. Kroening, T. B. Larsen, *Phys Earth Planet Int.* **77**, 205 (1993).
35. A. M. Jellinek, M. Manga, *Nature* **418**, 760 (2002).
36. B. Dupré, C. J. Allègre, *Nature* **303**, 142 (1983).
37. R. Montelli *et al.*, *Science* **303**, 338 (2004).
38. N. A. Simmons, A. M. Forte, S. P. Grand, *Earth Planet. Sci. Lett.* **246**, 109 (2006).
39. C. Reigber *et al.*, *J. Geodynamics* **39**, 1 (2005).
40. M. A. Richards, B. H. Hager, N. H. Sleep, *J. Geophys. Res.* **93**, 790 (1988).
41. M. A. Richards, D. C. Engebretson, *Nature* **355**, 437 (1992).
42. H.-P. Bunge, M. A. Richards, J. R. Baumgardner, *J. Geophys. Res.* **102**, 11,991 (1997).
43. A. Lenardic, M. A. Richards, F. H. Busse, *J. Geophys. Res.* **111**, B07404 (2006).
44. M. A. Richards, in *Glacial Isostasy, Sea Level and Mantle Rheology*, R. Sabadini, K. Lambeck, E. Boschi, Eds. (NATO ASI Ser. C, vol. 334, Kluwer, Norwell, MA, 1991), pp. 571–587.
45. N. H. Sleep, *C. R. Geosci.* **335**, 9 (2003).
46. H.-P. Bunge, M. A. Richards, J. R. Baumgardner, *Philos. Trans. R. Soc. Ser. A* **360**, 2545 (2002).
47. B. H. Hager, *J. Geophys. Res.* **89**, 6003 (1984).
48. J. P. Lowman, S. D. King, C. W. Gable, *Geochem. Geophys. Geosyst.* **5**, Q01101 (2004).
49. J. Besse, V. Courtillot, *J. Geophys. Res.* **107**, 2300 (2002).
50. M. A. Richards, H. P. Bunge, Y. Ricard, J. R. Baumgardner, *Geophys. Res. Lett.* **26**, 1777 (1999).
51. V. Courtillot, A. Davaille, J. Besse, J. Stock, *Earth Planet. Sci. Lett.* **205**, 295 (2003).
52. I. O. Norton, *Tectonics* **14**, 1080 (1995).
53. A. Piazzoni, G. Steinle-Neumann, H.-P. Bunge, D. Dolejš, *Geochem. Geophys. Geosyst.* **8**, Q11010 (2007).
54. H. P. Bunge, C. R. Hagelberg, B. J. Travis, *Geophys. J. Int.* **152**, 280 (2003).
55. We thank R. Cottrell and P. Doubrovine for discussions. This work was supported by the NSF.

10.1126/science.1161256